

New physics behind the new muon $g-2$ puzzle?

Luca Di Luzio,^{1,2} Antonio Masiero,^{1,2} Paride Paradisi,^{1,2} and Massimo Passera²

¹*Dipartimento di Fisica e Astronomia ‘G. Galilei’, Università di Padova, Italy*

²*Istituto Nazionale di Fisica Nucleare, Sezione di Padova, Padova, Italy*

The recent measurement of the muon $g-2$ at Fermilab confirms the previous Brookhaven result. The leading hadronic vacuum polarization (HVP) contribution to the muon $g-2$ represents a crucial ingredient to establish if the Standard Model prediction differs from the experimental value. A recent lattice QCD result by the BMW collaboration shows a tension with the low-energy $e^+e^- \rightarrow$ hadrons data which are currently used to determine the HVP contribution. We refer to this tension as the new muon $g-2$ puzzle. In this Letter we consider the possibility that new physics contributes to the $e^+e^- \rightarrow$ hadrons cross-section. This scenario could, in principle, solve the new muon $g-2$ puzzle. However, we show that this solution is excluded by a number of experimental constraints.

Introduction. The anomalous magnetic moment of the muon, $a_\mu \equiv (g_\mu - 2)/2$, has provided a persisting hint of new physics (NP) for many years. The recent a_μ measurement by the Muon $g-2$ collaboration at Fermilab [1–4] has confirmed the earlier result by the E821 experiment at Brookhaven [5], yielding the average $a_\mu^{\text{EXP}} = 116592061(41) \times 10^{-11}$. The comparison of this result with the Standard Model (SM) prediction $a_\mu^{\text{SM}} = 116591810(43) \times 10^{-11}$ of the Muon $g-2$ Theory Initiative [6] leads to an intriguing 4.2σ discrepancy [1]

$$\Delta a_\mu = a_\mu^{\text{EXP}} - a_\mu^{\text{SM}} = 251(59) \times 10^{-11}. \quad (1)$$

The expected forthcoming results of the Fermilab experiment plan to reach a sensitivity four-times better than the E821 one. Moreover, in a longer term, also the E34 collaboration at J-PARC [7] aims at measuring the muon $g-2$ through a new low-energy approach.

On the theory side, the only source of sizable uncertainties in a_μ^{SM} stems from the non-perturbative contributions of the hadronic sector, which have been under close scrutiny for several years. The SM prediction a_μ^{SM} in Eq. (1) has been derived using $(a_\mu^{\text{HVP}})^{\text{TI}}_{e^+e^-}$, the leading hadronic vacuum polarization (HVP) contribution to the muon $g-2$ based on low-energy $e^+e^- \rightarrow$ hadrons data obtained by the Muon $g-2$ Theory Initiative [6] (see also [8–28]). Alternatively, the HVP contribution has been computed using a first-principle lattice QCD approach [6] (see also [29–33]). Recently, the BMW lattice QCD collaboration (BMWc) computed the leading HVP contribution to the muon $g-2$ with sub per-cent precision, finding a value, $(a_\mu^{\text{HVP}})_{\text{BMW}}$, larger than $(a_\mu^{\text{HVP}})^{\text{TI}}_{e^+e^-}$ [34]. If $(a_\mu^{\text{HVP}})_{\text{BMW}}$ is used to obtain a_μ^{SM} instead of $(a_\mu^{\text{HVP}})^{\text{TI}}_{e^+e^-}$, the discrepancy with the experimental result is reduced to 1.6σ only. The above results are respectively

$$(a_\mu^{\text{HVP}})^{\text{TI}}_{e^+e^-} = 6931(40) \times 10^{-11}, \quad (2)$$

$$(a_\mu^{\text{HVP}})_{\text{BMW}} = 7075(55) \times 10^{-11}. \quad (3)$$

The present situation regarding the leading HVP contribution to the muon $g-2$ can be schematically represented as in Fig. 1, where $(a_\mu^{\text{HVP}})_{\text{EXP}}$ is the value of the HVP contribution required to exactly match a_μ^{EXP} assuming no

NP. Hereafter, the difference between the discrepancies in Fig. 1 will be referred to as the *new muon $g-2$ puzzle*.

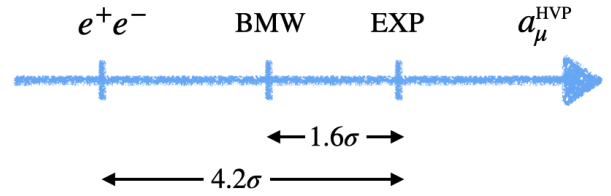


FIG. 1. The new muon $g-2$ puzzle: 4.2σ vs. 1.6σ .

Assuming that both $(a_\mu^{\text{HVP}})^{\text{TI}}_{e^+e^-}$ and $(a_\mu^{\text{HVP}})_{\text{BMW}}$ are correct, we ask whether this puzzle can be solved thanks to NP effects which would bring $(a_\mu^{\text{HVP}})^{\text{TI}}_{e^+e^-}$ in agreement with $(a_\mu^{\text{HVP}})_{\text{BMW}}$, *without* spoiling the 1.6σ agreement of $(a_\mu^{\text{HVP}})_{\text{BMW}}$ with $(a_\mu^{\text{HVP}})_{\text{EXP}}$. Differently from what has been usually done in the literature, here we do not assume a direct NP contribution to Δa_μ (i.e. new states that couple directly to muons). If fact, by itself this possibility could solve the longstanding discrepancy in Eq. (1), but not the new muon $g-2$ puzzle. Instead, in order to solve the latter, we invoke NP that modifies the $e^+e^- \rightarrow$ hadrons cross-section σ_{had} .

An increase of σ_{had} , due to an unforeseen missing contribution, has been already proposed to enhance $(a_\mu^{\text{HVP}})^{\text{TI}}_{e^+e^-}$ and solve Δa_μ [35–39]. However, the required shift in σ_{had} is disfavoured by the electroweak fit if it occurs at $\sqrt{s} \gtrsim 1$ GeV [37]. Hence, in the following, we will consider NP modifications of σ_{had} below the GeV scale. While Refs. [35–39] did not specify the origin of the shift in σ_{had} , we here assume that it is due to NP. After classifying in a model-independent way the general properties of such a NP, we investigate for the first time its non-trivial impact on e^+e^- and BMWc lattice results.

Crucial for our analysis is the dispersion relation used to determine $(a_\mu^{\text{HVP}})^{\text{TI}}_{e^+e^-}$ via σ_{had} . This relation follows from the application of the optical theorem to the photon HVP. It will be shown that scenarios in which NP couples only to hadrons are not able to solve the new muon $g-2$ puzzle. Instead, if NP couples both to hadrons and

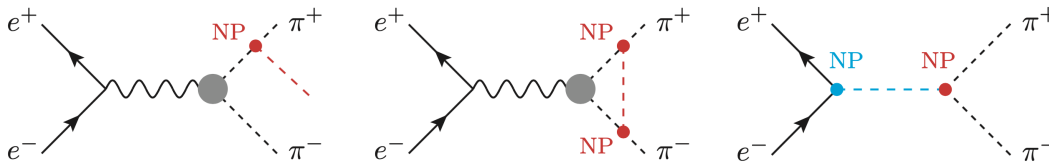


FIG. 2. Examples of NP contributions to σ_{had} via FSR (first and second diagram) and via a NP tree-level mediator coupled both to hadrons and electrons (third diagram).

electrons (and hence it contributes to σ_{had} at tree level), $(a_{\mu}^{\text{HVP}})_{e^+e^-}^{\text{TI}}$ should be subtracted of NP in the comparison with $(a_{\mu}^{\text{HVP}})_{\text{EXP}}$, whereas $(a_{\mu}^{\text{HVP}})_{\text{BMW}}$ should not. In fact, in this case, the quantity that should enter the dispersion relation determining the HVP contribution should not be the experimentally measured cross-section σ_{had} , but rather $\sigma_{\text{had}} - \Delta\sigma_{\text{had}}^{\text{NP}}$. Therefore, the tension between $(a_{\mu}^{\text{HVP}})_{e^+e^-}^{\text{TI}}$ and $(a_{\mu}^{\text{HVP}})_{\text{BMW}}$ could be solved by invoking a negative interference between the SM and NP, that is $\Delta\sigma_{\text{had}}^{\text{NP}} < 0$. As we will show below, the above picture selects a very specific NP scenario which entails new light particles with a mass scale $\lesssim 1$ GeV coupling to SM fermions through a vector current.

Model-independent analysis. Hereafter we are going to examine the general properties of NP models aiming at solving the new muon $g-2$ puzzle via a modification of σ_{had} . To this end, we introduce the dispersion relation

$$(a_{\mu}^{\text{HVP}})_{e^+e^-} = \frac{\alpha}{\pi^2} \int_{m_{\pi^0}^2}^{\infty} \frac{ds}{s} K(s) \text{Im} \Pi_{\text{had}}(s), \quad (4)$$

where $K(s)$ is a positive-definite kernel function with $K(s) \approx m_{\mu}^2/3s$ for $\sqrt{s} \gg m_{\mu}$. This equation defines the HVP contribution to the muon $g-2$ in terms of the photon HVP, Π_{had} , which includes possible NP effects. If the possible NP entering the photon HVP does not couple to electrons, i.e. it does not enter the hadronic cross-section at tree level, then Eq. (4) can be written as

$$(a_{\mu}^{\text{HVP}})_{e^+e^-} = \frac{1}{4\pi^3} \int_{m_{\pi^0}^2}^{\infty} ds K(s) \sigma_{\text{had}}(s), \quad (5)$$

where σ_{had} includes final-state radiation (FSR), whereas both vacuum polarization and initial-state radiation (ISR) effects are subtracted. In particular, vacuum polarization corrections can be simply accounted for by multiplying the experimental cross-section by $|\alpha/\alpha(s)|^2$, while the correction of ISR and ISR/FSR interference effects is addressed by each experimental collaboration. In this Letter we will focus on the region where σ_{had} is experimentally determined, i.e. $\sqrt{s} \gtrsim 0.3$ GeV, since this gives the by far dominant contribution to the dispersive integral in Eq. (5).

In Fig. 2 we show a schematic classification of how NP can enter σ_{had} . The first two diagrams are representative of FSR effects, which also unavoidably affect the photon HVP at the next-to-leading order (NLO). We can

safely neglect possible NP contaminations in ISR since the bounds on NP couplings to electrons are very severe. The third diagram, where NP enters the hadronic cross-section at tree level coupling both to hadrons and electrons, is due to NP that also modifies the photon HVP at NLO. Crucially, however, its dominant contribution to the muon $g-2$ emerges via the tree-level shift of σ_{had} .

Hence, when invoking NP in σ_{had} , there are two different scenarios to be considered, depending on whether NP couples only to hadrons or both to hadrons and electrons. In the following, we analyze these two possibilities and their capability to solve the new muon $g-2$ puzzle.

1. NP coupled only to hadrons. This scenario is schematically represented by the first two diagrams of Fig. 2. As remarked above, real and virtual FSR must be included in σ_{had} . However, in order to establish the impact of NP in FSR (which depends on the interplay between the mass scale of NP and the experimental cuts), it would be mandatory to perform dedicated experimental analyses imposing the various selection cuts specific of each experimental setup, which is beyond the scope of this Letter. Since the full photon FSR effect estimated in scalar QED amounts only to 50×10^{-11} [6, 40], a value well below the discrepancy between Eqs. (2)–(3), and given that light NP couplings with the SM particles are tightly constrained, the NP contributions in FSR cannot solve the new muon $g-2$ puzzle.

2. NP coupled both to hadrons and electrons. If NP contributes to σ_{had} at tree level (see third diagram in Fig. 2), then only the subtracted cross-section $\sigma_{\text{had}} - \Delta\sigma_{\text{had}}^{\text{NP}}$ should be included in Eq. (5). We note that the latter can be larger than σ_{had} if $\Delta\sigma_{\text{had}}^{\text{NP}} < 0$, thus requiring that the NP contribution is dominated by a *negative* interference with the SM. As $(a_{\mu}^{\text{HVP}})_{e^+e^-}^{\text{TI}}$ has been computed using σ_{had} rather than the subtracted cross-section $\sigma_{\text{had}} - \Delta\sigma_{\text{had}}^{\text{NP}}$, the theoretical prediction of the HVP contribution in Eq. (5) is

$$(a_{\mu}^{\text{HVP}})_{e^+e^-} = (a_{\mu}^{\text{HVP}})_{e^+e^-}^{\text{TI}} + (a_{\mu}^{\text{HVP}})_{\text{NP}}, \quad (6)$$

where $(a_{\mu}^{\text{HVP}})_{\text{NP}}$ describes NP effects at LO, due to the tree-level exchange of the NP mediator (see third diagram in Fig. 2), as well as at NLO. Instead, $(a_{\mu}^{\text{HVP}})_{\text{BMW}}$ should be shifted only by NLO NP effects. Remarkably, this scenario may allow to match Eq. (6) with $(a_{\mu}^{\text{HVP}})_{\text{EXP}}$, while keeping at the same time the agreement with the BMWc lattice result.

Light new physics analysis. We now explore whether the second scenario envisaged above can be quantitatively realized in an explicit NP model. Motivated by the fact that the kernel function in Eq. (5) scales like $1/s$ and by the fact that modifications of σ_{had} above ~ 1 GeV are disfavoured by electroweak precision tests [37], we focus on the sub-GeV energy range, where the dominant contribution to σ_{had} arises from the $e^+e^- \rightarrow \pi^+\pi^-$ channel. In fact, in the SM, this channel accounts for more than 70% of the full hadronic contribution to the muon $g-2$. Furthermore, the requirement of having a sizeable negative interference with the SM amplitude narrows down the general class of NP models. Indeed, the interference of scalar couplings with the SM vector current is suppressed by the electron mass, while pseudoscalar and axial couplings do not interfere. Hence, we focus on the tree-level exchange of a light Z' boson with the following vector couplings to electrons and first-generation quarks¹

$$\mathcal{L}_{Z'} \supset (g_V^e \bar{e}\gamma^\mu e + g_V^q \bar{q}\gamma^\mu q)Z'_\mu, \quad (7)$$

with $q = u, d$ and $m_{Z'} \lesssim 1$ GeV.

The matrix element of the two-pion intermediate state can be expressed in terms of the pion vector form factor

$$\langle \pi^\pm(p') | J_{\text{em}}^\mu(0) | \pi^\pm(p) \rangle = \pm(p' + p)^\mu F_\pi^V(q^2), \quad (8)$$

where $q = p' - p$ and $J_{\text{em}}^\mu = \frac{2}{3}\bar{u}\gamma^\mu u - \frac{1}{3}\bar{d}\gamma^\mu d$ is the electromagnetic current. Exploiting the charge conjugation invariance, in the iso-spin symmetric limit, we find that

$$\langle \pi^\pm | J_{\text{em}}^\mu | \pi^\pm \rangle = \langle \pi^\pm | \bar{u}\gamma^\mu u | \pi^\pm \rangle = -\langle \pi^\pm | \bar{d}\gamma^\mu d | \pi^\pm \rangle. \quad (9)$$

Hence, $F_\pi^V(q^2)$ also describes the matrix element of the Z' quark current $J_{Z'}^\mu = g_V^u \bar{u}\gamma^\mu u + g_V^d \bar{d}\gamma^\mu d$

$$\langle \pi^\pm(p') | J_{Z'}^\mu(0) | \pi^\pm(p) \rangle = \pm(p' + p)^\mu F_\pi^V(q^2)(g_V^u - g_V^d). \quad (10)$$

Note that if the Z' interactions are iso-spin symmetric, then $g_V^u = g_V^d$ and the contribution to the $\pi^+\pi^-$ amplitude vanishes. Defining $\sigma_{\pi\pi}^{\text{SM+NP}} = \sigma_{\pi\pi}^{\text{SM}} + \Delta\sigma_{\pi\pi}^{\text{NP}}$, the tree-level exchange of the Z' with width $\Gamma_{Z'}$ leads to

$$\frac{\sigma_{\pi\pi}^{\text{SM+NP}}}{\sigma_{\pi\pi}^{\text{SM}}} = \left| 1 + \frac{g_V^e(g_V^u - g_V^d)}{e^2} \frac{s}{s - m_{Z'}^2 + im_{Z'}\Gamma_{Z'}} \right|^2, \quad (11)$$

where the pion vector form factor cancels out in the ratio.

The dispersive contribution to the muon $g-2$ due to SM and NP can be obtained by using $\sigma_{\text{had}} - \Delta\sigma_{\text{had}}^{\text{NP}}$ in Eq. (5). Imposing that the current discrepancy Δa_μ is solved by NP in the hadronic cross-section, we obtain

$$\Delta a_\mu = \frac{1}{4\pi^3} \int_{s_{\text{exp}}}^{\infty} ds K(s) (-\Delta\sigma_{\text{had}}^{\text{NP}}(s)), \quad (12)$$

¹ Assuming only the interactions in Eq. (7), the gauge current associated to the Z' would be anomalous. Additional heavy fermions charged under the electroweak group can be introduced in order to make the model UV consistent.

where the lower integration limit is $s_{\text{exp}} \approx (0.3 \text{ GeV})^2$, that is, the integral is performed in the data-driven region for the $\pi\pi$ channel. Approximating $\Delta\sigma_{\text{had}}^{\text{NP}} \approx \Delta\sigma_{\pi\pi}^{\text{NP}}$,² from Eq. (11) we find

$$\Delta\sigma_{\text{had}}^{\text{NP}}(s) \approx \sigma_{\pi\pi}^{\text{SM}}(s) \times \frac{2\epsilon s(s - m_{Z'}^2) + \epsilon^2 s^2}{(s - m_{Z'}^2)^2 + m_{Z'}^4 \gamma^2}, \quad (13)$$

where we introduced the effective coupling $\epsilon \equiv g_V^e(g_V^u - g_V^d)/e^2$ and the adimensional width parameter $\gamma \equiv \Gamma_{Z'}/m_{Z'}$. If both the $Z' \rightarrow ee$ and $Z' \rightarrow \pi^+\pi^-$ channels are kinematically open, the associated decay widths (normalized to $m_{Z'}$) read, respectively

$$\gamma_{ee} \approx \frac{(g_V^e)^2}{12\pi} = 2.7 \times 10^{-10} \left(\frac{g_V^e}{10^{-4}} \right)^2, \quad (14)$$

up to $(m_e/m_{Z'})^4$ corrections, and

$$\gamma_{\pi\pi} = \frac{(g_V^u - g_V^d)^2}{48\pi} |F_\pi^V(m_{Z'}^2)|^2 \left(1 - \frac{4m_\pi^2}{m_{Z'}^2} \right)^{3/2}, \quad (15)$$

where $|F_\pi^V(m_{Z'}^2)|^2$ (normalized to $F_\pi^V(0) = 1$) can be enhanced up to a factor of 45 by the ρ resonance [11]. For $m_{Z'} < 2m_{\pi^+} \approx 0.28$ GeV, $\gamma = \gamma_{ee}$, whereas for $m_{Z'} \in [0.3, 1]$ GeV we can approximate $\gamma \approx \gamma_{\pi\pi}$ since the e^+e^- channel can be safely neglected given the tight bounds on g_V^e . Note that possible contributions to γ stemming from non-SM final states (e.g. decays into a dark sector) yield a positive-definite shift to σ_{had} , since they cannot interfere with the SM. Hence, they contribute with a negative shift to Δa_μ (cf. Eq. (12)), thus worsening the discrepancy.

² We expect that this approximation reproduces Δa_μ with $\mathcal{O}(20)\%$ accuracy. Indeed, in the SM, the $\pi^0\gamma$ and $n\pi$ channels (with $n > 2$) amount to 17% of the $\pi\pi$ channel contribution to $(a_\mu^{\text{HVP}})_{e^+e^-}^{\text{PI}}$ (see e.g. [14]). Moreover, NP is assumed to couple only to up and down quarks so that the contribution of other heavy mesons is negligible.

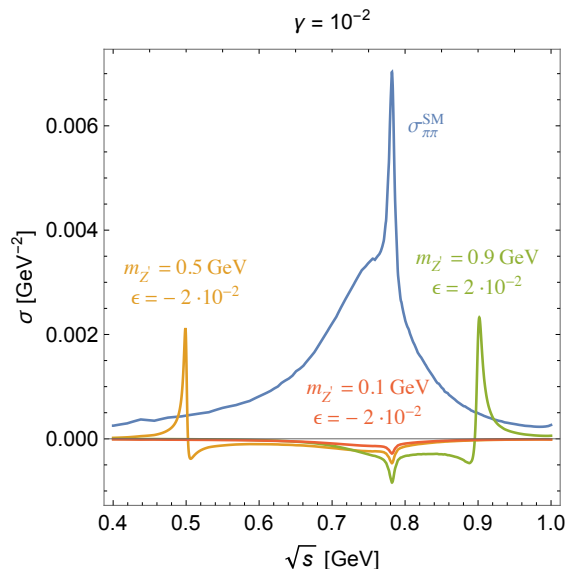


FIG. 3. $\sigma_{\text{had}}^{\text{SM}}$ and $\Delta\sigma_{\text{had}}^{\text{NP}}$ for some benchmark values of the Z' model parameters solving the Δa_μ discrepancy, see Eq. (1).

The profile of $\Delta\sigma_{\text{had}}^{\text{NP}}$, together with its SM counterpart (taken from Ref. [14]), is shown in Fig. 3 for some representative benchmark values of the Z' model parameters addressing the Δa_μ discrepancy. In particular, we find that Z' masses below the ρ resonance require $\epsilon < 0$, whereas Z' masses above it require $\epsilon > 0$. Moreover, in order to obtain $\Delta a_\mu > 0$, the interference term has to dominate over the pure resonant effect in Eq. (13). All in all, we find that the parameters of the Z' model that are needed to explain Δa_μ can be divided in two regions: *i*) $m_{Z'} \gtrsim 0.3$ GeV which requires $|\epsilon| \approx 10^{-2}$ and $\gamma \gtrsim 10^{-3}$ and *ii*) $m_{Z'} \lesssim 0.3$ GeV which requires $|\epsilon| \approx 10^{-2}$ and basically no relevant constraint on γ (as evident from Eq. (13)). We note that in principle it could be possible to directly observe (with a dedicated scanning analysis) the new resonance in e^+e^- data for particular choices of the Z' mass and width parameters. However, since there are also configurations that can explain Δa_μ with a very narrow and light Z' below the experimental resolution, it still remains necessary to constrain the Z' couplings indirectly.

In the following, we are going to inspect whether the region of the parameter space of the Z' model needed to explain Δa_μ is allowed by experimental constraints. These can be divided for convenience in three classes: 1. semi-leptonic processes; 2. purely leptonic processes and 3. purely hadronic, iso-spin violating observables.

1. Semi-leptonic processes. The $e^+e^- \rightarrow q\bar{q}$ cross-section, σ_{qq} , has been measured with a per-cent level accuracy at LEP II for center of mass energies $\sqrt{s} \in [130, 207]$ GeV [41]. The leading effect to this process

induced by a Z' exchange is given by

$$\frac{\sigma_{qq}^{\text{SM+NP}}}{\sigma_{qq}^{\text{SM}}} \approx 1 + 2 \frac{g_V^e g_V^q}{e^2 Q_q}, \quad (16)$$

where Q_q denotes the quark charge. Requiring that the deviation from unity in Eq. (16) is less than 1% [41] leads to $|g_V^e g_V^q| \lesssim 4.6 \cdot 10^{-4} |Q_q|$ which translates into $\epsilon \lesssim 3.3 \cdot 10^{-3}$. Moreover, the bound does not depend on the Z' mass and it acts on a coupling combination that is similar to the one entering $\Delta\sigma_{\pi\pi}^{\text{NP}}$, but not vanishing in the iso-spin symmetric limit $g_V^u = g_V^d$. Hence, this bound can be considered to be conservative.

2. Leptonic processes. The Z' coupling to electrons is also tightly constrained. In particular, the non-observation at BaBar of the process $e^+e^- \rightarrow \gamma Z'$ followed by the decay $Z' \rightarrow e^+e^-$ yields $g_V^e \lesssim 2 \cdot 10^{-4}$ [42] if the Z' decays dominantly into electrons. Therefore, in our framework, this bound applies only for $m_{Z'} \lesssim 0.3$ GeV where the $Z' \rightarrow \pi^+\pi^-$ decay is not kinematically allowed. Moreover, another important bound arises from the electron $g-2$, yielding $|g_V^e| \lesssim 10^{-2} (m_{Z'}/0.5 \text{ GeV})$ for $m_{Z'} \gtrsim \text{MeV}$.

3. Iso-spin breaking observables. The Z' contribution to $\Delta\sigma_{\pi\pi}^{\text{NP}}$ is proportional to the iso-spin breaking combination $g_V^u - g_V^d$, which should be of $\mathcal{O}(1)$ in order to explain Δa_μ in the $m_{Z'} \gtrsim 0.3$ GeV region. Therefore, it is natural to expect sizeable effects on other iso-spin violating hadronic observables. A relevant example is given by the charged vs. neutral pion mass squared difference, $\Delta m^2 = m_{\pi^+}^2 - m_{\pi^0}^2$. Analogously to the QED case, the quadratically divergent Z' loop leads to

$$(\Delta m^2)_{Z'} \sim \frac{(g_V^u - g_V^d)^2}{(4\pi)^2} \Lambda_\chi^2, \quad (17)$$

where $\Lambda_\chi \approx 1$ GeV is the cut-off scale of the chiral theory and we chose $m_{Z'} \ll \Lambda_\chi$. Instead, for $m_{Z'} \gg \Lambda_\chi$, the Z' contribution to Δm^2 decouples as $\Lambda_\chi^2/m_{Z'}^2 \ll 1$. In practice, the NP contribution from a light Z' is more reliably obtained by rescaling the SM prediction from lattice QCD [43] with $(g_V^u - g_V^d)^2/e^2$. Then, comparing the SM prediction of Δm^2 with its experimental value, we find the 95% C.L. bound $|g_V^u - g_V^d| \lesssim 0.06$.

The interplay of the above constraints in the plane $-g_V^e$ vs. $g_V^u - g_V^d$ is displayed in Fig. 4 for two representative scenarios where $m_{Z'} = 0.1$ and 0.5 GeV. The directions of the arrows indicate the excluded regions by the different experimental bounds. Instead, the red band is the region favoured by the explanation of the muon $g-2$ discrepancy. From Fig. 4 it is clear that, irrespectively of the Z' mass, there are always at least two independent bounds preventing to solve the new muon $g-2$ puzzle.

Conclusions. The recent lattice QCD result by the BMW collaboration shows a tension with the low-energy $e^+e^- \rightarrow$ hadrons data currently used to determine the

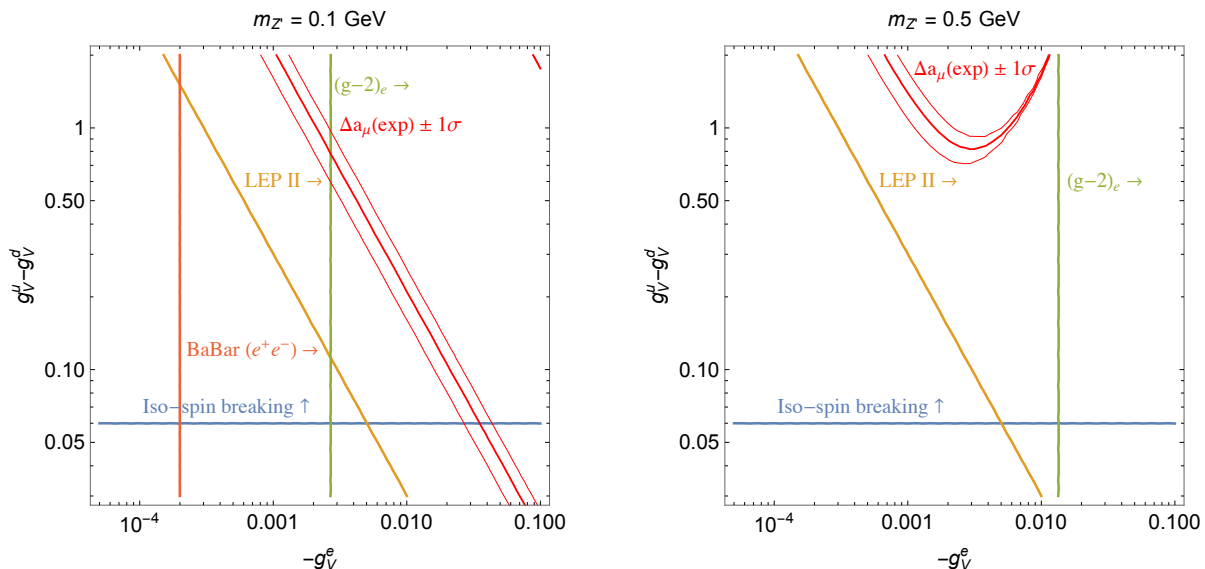


FIG. 4. Z' contribution to Δa_μ via a modification of σ_{had} vs. Z' constraints.

HVP contribution to the muon $g-2$. In this Letter we investigated the possibility to solve this tension, referred to as the *new muon $g-2$ puzzle*, invoking NP in the hadronic cross-section. A possible way to restore full consistency into the picture is to postulate a *negative* shift in σ_{had} due to NP. We showed that this scenario requires the presence of a light NP mediator that modifies the experimental cross-section σ_{had} . However, this non-trivial setup, where NP hides in $e^+e^- \rightarrow \text{hadrons}$ data, is excluded by a number of experimental constraints. Alternative confirmations of the e^+e^- determinations of the HVP contribution to the muon $g-2$, based on either additional lattice QCD calculations or direct experimental measurements, as proposed by the MUonE experiment [44–46],³ will hence be crucial to shed light on this intriguing puzzle.

Note added. After this paper was posted on the arXiv, Ref. [49] appeared in which the authors studied the possibility of reconciling the data driven and the BMWc lattice determinations of a_μ^{HVP} by rescaling the KLOE luminosity via a NP contribution to Bhabha scattering. Hence, contrary to our analysis, in their approach NP does not directly contribute to σ_{had} .

Acknowledgments. We thank M. Fael, A. Keshavarzi, L. Vecchi and G. Venanzoni for helpful discussions. This work was partially supported by the European Union’s Horizon 2020 research and innovation programme under the Marie Skłodowska-Curie grant agreement No 860881-HIDDEN, by the research grant “The Dark Universe: A Synergic Multi-messenger Approach” number

2017X7X85K under the program PRIN 2017 funded by the Ministero dell’Istruzione, Università e della Ricerca (MIUR) and by the INFN Iniziative Specifiche APINE and TASP.

-
- [1] B. Abi *et al.* (Muon $g-2$), *Phys. Rev. Lett.* **126**, 141801 (2021), arXiv:2104.03281 [hep-ex].
 - [2] T. Albahri *et al.* (Muon $g-2$), *Phys. Rev. D* **103**, 072002 (2021), arXiv:2104.03247 [hep-ex].
 - [3] T. Albahri *et al.* (Muon $g-2$), *Phys. Rev. A* **103**, 042208 (2021), arXiv:2104.03201 [hep-ex].
 - [4] T. Albahri *et al.* (Muon $g-2$), *Phys. Rev. Accel. Beams* **24**, 044002 (2021), arXiv:2104.03240 [physics.acc-ph].
 - [5] G. W. Bennett *et al.* (Muon $g-2$), *Phys. Rev. D* **73**, 072003 (2006), arXiv:hep-ex/0602035.
 - [6] T. Aoyama *et al.*, *Phys. Rept.* **887**, 1 (2020), arXiv:2006.04822 [hep-ph].
 - [7] M. Abe *et al.*, *PTEP* **2019**, 053C02 (2019), arXiv:1901.03047 [physics.ins-det].
 - [8] F. Jegerlehner, *The Anomalous Magnetic Moment of the Muon*, Vol. 274 (Springer, Cham, 2017).
 - [9] M. Davier, A. Hoecker, B. Malaescu, and Z. Zhang, *Eur. Phys. J. C* **77**, 827 (2017), arXiv:1706.09436 [hep-ph].
 - [10] A. Keshavarzi, D. Nomura, and T. Teubner, *Phys. Rev. D* **97**, 114025 (2018), arXiv:1802.02995 [hep-ph].
 - [11] G. Colangelo, M. Hoferichter, and P. Stoffer, *JHEP* **02**, 006 (2019), arXiv:1810.00007 [hep-ph].
 - [12] M. Hoferichter, B.-L. Hoid, and B. Kubis, *JHEP* **08**, 137 (2019), arXiv:1907.01556 [hep-ph].
 - [13] M. Davier, A. Hoecker, B. Malaescu, and Z. Zhang, *Eur. Phys. J. C* **80**, 241 (2020), [Erratum: *Eur.Phys.J.C* **80**, 410 (2020)], arXiv:1908.00921 [hep-ph].
 - [14] A. Keshavarzi, D. Nomura, and T. Teubner, *Phys. Rev. D* **101**, 014029 (2020), arXiv:1911.00367 [hep-ph].
 - [15] B.-L. Hoid, M. Hoferichter, and B. Kubis, *Eur. Phys. J. C* **80**, 988 (2020), arXiv:2007.12696 [hep-ph].

³ It is very unlikely that NP contributions will contaminate the MUonE’s extraction of a_μ^{HVP} [47, 48].

- [16] A. Kurz, T. Liu, P. Marquard, and M. Steinhauser, *Phys. Lett. B* **734**, 144 (2014), [arXiv:1403.6400 \[hep-ph\]](#).
- [17] K. Melnikov and A. Vainshtein, *Phys. Rev. D* **70**, 113006 (2004), [arXiv:hep-ph/0312226](#).
- [18] P. Masjuan and P. Sanchez-Puertas, *Phys. Rev. D* **95**, 054026 (2017), [arXiv:1701.05829 \[hep-ph\]](#).
- [19] G. Colangelo, M. Hoferichter, M. Procura, and P. Stoffer, *JHEP* **04**, 161 (2017), [arXiv:1702.07347 \[hep-ph\]](#).
- [20] M. Hoferichter, B.-L. Hoid, B. Kubis, S. Leupold, and S. P. Schneider, *JHEP* **10**, 141 (2018), [arXiv:1808.04823 \[hep-ph\]](#).
- [21] A. Gérardin, H. B. Meyer, and A. Nyffeler, *Phys. Rev. D* **100**, 034520 (2019), [arXiv:1903.09471 \[hep-lat\]](#).
- [22] J. Bijnens, N. Hermansson-Truedsson, and A. Rodríguez-Sánchez, *Phys. Lett. B* **798**, 134994 (2019), [arXiv:1908.03331 \[hep-ph\]](#).
- [23] G. Colangelo, F. Hagelstein, M. Hoferichter, L. Laub, and P. Stoffer, *JHEP* **03**, 101 (2020), [arXiv:1910.13432 \[hep-ph\]](#).
- [24] T. Blum, N. Christ, M. Hayakawa, T. Izubuchi, L. Jin, C. Jung, and C. Lehner, *Phys. Rev. Lett.* **124**, 132002 (2020), [arXiv:1911.08123 \[hep-lat\]](#).
- [25] T. Aoyama, M. Hayakawa, T. Kinoshita, and M. Nio, *Phys. Rev. Lett.* **109**, 111808 (2012), [arXiv:1205.5370 \[hep-ph\]](#).
- [26] T. Aoyama, T. Kinoshita, and M. Nio, *Atoms* **7**, 28 (2019).
- [27] A. Czarnecki, W. J. Marciano, and A. Vainshtein, *Phys. Rev. D* **67**, 073006 (2003), [Erratum: *Phys. Rev. D* **73**, 119901 (2006)], [arXiv:hep-ph/0212229](#).
- [28] C. Gnendiger, D. Stöckinger, and H. Stöckinger-Kim, *Phys. Rev. D* **88**, 053005 (2013), [arXiv:1306.5546 \[hep-ph\]](#).
- [29] S. Borsanyi *et al.* (Budapest-Marseille-Wuppertal), *Phys. Rev. Lett.* **121**, 022002 (2018), [arXiv:1711.04980 \[hep-lat\]](#).
- [30] T. Blum, P. A. Boyle, V. Gülpers, T. Izubuchi, L. Jin, C. Jung, A. Jüttner, C. Lehner, A. Portelli, and J. T. Tsang (RBC, UKQCD), *Phys. Rev. Lett.* **121**, 022003 (2018), [arXiv:1801.07224 \[hep-lat\]](#).
- [31] D. Giusti, V. Lubicz, G. Martinelli, F. Sanfilippo, and S. Simula, *Phys. Rev. D* **99**, 114502 (2019), [arXiv:1901.10462 \[hep-lat\]](#).
- [32] C. T. H. Davies *et al.* (Fermilab Lattice, LATTICE-HPQCD, MILC), *Phys. Rev. D* **101**, 034512 (2020), [arXiv:1902.04223 \[hep-lat\]](#).
- [33] A. Gérardin, M. Cè, G. von Hippel, B. Hörz, H. B. Meyer, D. Mohler, K. Ottnad, J. Wilhelm, and H. Wittig, *Phys. Rev. D* **100**, 014510 (2019), [arXiv:1904.03120 \[hep-lat\]](#).
- [34] S. Borsanyi *et al.*, *Nature* **593**, 51 (2021), [arXiv:2002.12347 \[hep-lat\]](#).
- [35] M. Passera, W. J. Marciano, and A. Sirlin, *Phys. Rev. D* **78**, 013009 (2008), [arXiv:0804.1142 \[hep-ph\]](#).
- [36] A. Crivellin, M. Hoferichter, C. A. Manzari, and M. Montull, *Phys. Rev. Lett.* **125**, 091801 (2020), [arXiv:2003.04886 \[hep-ph\]](#).
- [37] A. Keshavarzi, W. J. Marciano, M. Passera, and A. Sirlin, *Phys. Rev. D* **102**, 033002 (2020), [arXiv:2006.12666 \[hep-ph\]](#).
- [38] B. Malaescu and M. Schott, *Eur. Phys. J. C* **81**, 46 (2021), [arXiv:2008.08107 \[hep-ph\]](#).
- [39] G. Colangelo, M. Hoferichter, and P. Stoffer, *Phys. Lett. B* **814**, 136073 (2021), [arXiv:2010.07943 \[hep-ph\]](#).
- [40] J. S. Schwinger, *Particles, Sources, and Fields. Vol. 3* (1989).
- [41] S. Schael *et al.* (ALEPH, DELPHI, L3, OPAL, LEP Electroweak), *Phys. Rept.* **532**, 119 (2013), [arXiv:1302.3415 \[hep-ex\]](#).
- [42] J. P. Lees *et al.* (BaBar), *Phys. Rev. Lett.* **113**, 201801 (2014), [arXiv:1406.2980 \[hep-ex\]](#).
- [43] R. Frezzotti, G. Gagliardi, V. Lubicz, G. Martinelli, F. Sanfilippo, and S. Simula, *38th International Symposium on Lattice Field Theory*, (2021), [arXiv:2112.01066 \[hep-lat\]](#).
- [44] C. M. Carloni Calame, M. Passera, L. Trentadue, and G. Venanzoni, *Phys. Lett. B* **746**, 325 (2015), [arXiv:1504.02228 \[hep-ph\]](#).
- [45] G. Abbiendi *et al.*, *Eur. Phys. J. C* **77**, 139 (2017), [arXiv:1609.08987 \[hep-ex\]](#).
- [46] G. Abbiendi *et al.*, “Letter of Intent: The MUonE Project, CERN-SPSC-2019-026 / SPSC-I-252,” (2019), <http://cds.cern.ch/record/2677471/files/SPSC-I-252.pdf?version=1>.
- [47] P. S. B. Dev, W. Rodejohann, X.-J. Xu, and Y. Zhang, *JHEP* **05**, 053 (2020), [arXiv:2002.04822 \[hep-ph\]](#).
- [48] A. Masiero, P. Paradisi, and M. Passera, *Phys. Rev. D* **102**, 075013 (2020), [arXiv:2002.05418 \[hep-ph\]](#).
- [49] L. Darmé, G. G. di Cortona, and E. Nardi, (2021), [arXiv:2112.09139 \[hep-ph\]](#).